DOI: 10.1002/chem.200903131

$BF_3 \cdot OEt_2$-Catalyzed Intermolecular Reactions of Vinylidenecyclopropanes with Bis(*p*-alkoxyphenyl)methanols: A Novel Cationic 1,4-Aryl-Migration Process

Lei Wu, Min Shi,* and Yuxue Li*[a]

Abstract: $BF_3 \cdot OEt_2$-catalyzed reactions of vinylidenecyclopropanes (VDCPs) **1** with bis(aryl)methanols **2** were thoroughly investigated. When VDCPs **1** reacted with electron-rich bis(aryl)methanols **2**, diastereomeric rotamers of indene derivatives formed in excellent yields by a novel cationic 1,4-aryl migration between two carbon atoms and the subsequent intramolecular Friedel–Crafts reaction pathways in the presence of $BF_3 \cdot OEt_2$ under mild conditions. As for electron-deficient or less-electron-rich bis(aryl)methanols **2**, either trialkene products formed in good yields by direct deprotonation, or another type of indene derivative was produced by direct intramolecular Friedel–Crafts reaction, depending on the substituents on the cyclopropane of VDCPs. In addition, DFT calculations were carried out to explain the experimental results. Plausible mechanisms for all these transformations are proposed on the basis of the experimental and computational results.

Keywords: allenes · aryl migration · carbocatios · density functional calculations · diastereomeric rotamers · Friedel–Crafts reaction

Introduction

Vinylidenecyclopropanes (VDCPs),[1] containing an allene moiety and a connected cyclopropane ring, belong to the most remarkable organic families in the chemistry of highly strained small rings. These highly strained cyclopropanes are thermally stable, yet reactive substances, which easily undergo novel intramolecular rearrangements or intermolecular reactions with many electrophiles, either upon heating and photoirradiation, or catalyzed by a variety of Lewis or Brønsted acids. For example, VDCPs can react with carbon–carbon or carbon–heteroatom multiple bonds to produce [3+2] or [2+2] cycloaddition products in good yields upon heating or photoirradiation.[2] Moreover, very recently, we and others have reported Lewis acid or Brønsted acid catalyzed/mediated [3+2] or [3+3] cycloaddition reactions of VDCPs with imines, aldehydes, nitriles, α,β-unsaturated ketones, and so forth, to give the corresponding functionalized tetrahydrofuran and 3,6-dihydropyran derivatives as well as some other cycloadducts in moderate to good yields under mild conditions.[3–5] All these interesting results have stimulated us to further explore such cascade ring-opening reactions of VDCPs in the presence of other electrophiles catalyzed by Lewis acids.

During our ongoing investigation on the reactions of VDCPs with some electrophiles catalyzed by Lewis acids, we found that bis(aryl)methanols **2** could act as excellent precursors of electrophiles, affording active cationic intermediates to initiate the reactions with VDCPs **1**. Interestingly, a novel cationic 1,4-aryl migration from carbon atom to carbon atom in the presence of $BF_3 \cdot OEt_2$ was observed if electron-rich bis(*p*-alkoxyphenyl)methanols were used as the electrophiles under mild conditions (Scheme 1). Furthermore, we also found that if electron-deficient or less-electron-rich bis(aryl)methanols were used as the electrophiles, two other kinds of products were obtained by different reaction pathways, depending on the substituents on the cyclopropane of the substrates. More specifically, this interesting 1,4-aryl migration is highly dependent on the electronic nature of the bis(aryl)methanols employed, as well as the substituents on the cyclopropane of VDCPs. To gain more

[a] L. Wu, Prof. Dr. M. Shi, Prof. Dr. Y. Li
State Key Laboratory of Organometallic Chemistry
Shanghai Institute of Organic Chemistry
Chinese Academy of Sciences
354 Fenglin Road, Shanghai 200032 (China)
Fax: (+86) 21-64166128
E-mail: mshi@mail.sioc.ac.cn

Supporting information for this article is available from the author or on the WWW under http://dx.doi.org/10.1002/chem.200903131. It contains spectroscopic data of all the new compounds shown in Tables 1–5; detailed descriptions of the experimental procedures; X-ray data for compounds **3aA**, **3eB**, **6a**, and **7e**; the optimized structures in Figure 6; and the total energies and geometrical coordinates of the structures in Scheme 2 and Figure 7.

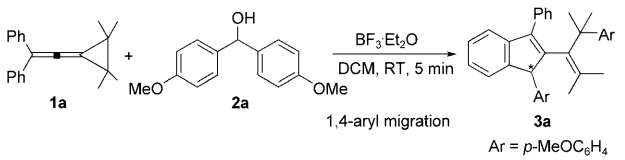

Scheme 1. $BF_3{\cdot}OEt_2$-catalyzed reactions of VDCP **1a** with bis(*p*-methoxyphenyl)methanol (**2a**).

insight into the reaction mechanisms and the related transition states, DFT calculations were carried out to explain the experimental results. On the basis of the results thus obtained, plausible reaction mechanisms were deduced, and these are described in this paper.

Regarding aryl migration,[6] besides the most extensively investigated 1,2-aryl migration (neophyl rearrangement),[7] 1,4-aryl-migration reactions have been also observed and studied. It has been known that this migration can take place between two carbon atoms, or between a carbon atom and a heteroatom, as well as between two heteroatoms. However, most of the 1,4-aryl-migration reactions proceed by a radical mechanism.[8] The examples concerning a cationic intermediate are rare.[9] Herein, we wish to report the full details of these interesting findings.

Results and Discussion

$BF_3{\cdot}OEt_2$-catalyzed reactions of VDCP 1a with bis(*p*-methoxyphenyl)methanol 2a: First, the reaction was carried out by using VDCP **1a** (0.20 mmol) and bis(*p*-methoxyphenyl)methanol (**2a**; 0.24 mmol, 1.2 equiv) in dichloromethane (2.0 mL) at room temperature (20 °C) in the presence of $BF_3{\cdot}OEt_2$ (10 mol %). The reaction was completed within 5 minutes to afford product **3a** as a pair of diastereomeric rotamers **3aA** and **3aB** in 73 % yield in a ratio of 8.1:1.0 (Table 1, entry 1). The structure of the major rotamer **3aA** was determined by X-ray diffraction (the CIF data are presented in the Supporting Information).[10] The ORTEP drawing is shown in Figure 1. It can be seen that one of the *p*-methoxyphenyl rings of **2a** has migrated to the ring-opened dimethyl site to give the product **3a**.

Next, we attempted to determine the best reaction conditions for this reaction, and the results of these experiments are summarized in Table 1. Examination of the solvent effects when $BF_3{\cdot}OEt_2$ (10 mol %) was used as the catalyst revealed that 1,2-dichloroethane (DCE) was the solvent of choice, affording **3a** in 96 % total yield (Table 1, entries 1 to 4). When other Lewis acids such as $[Sc(OTf)_3]$, $[Zr(OTf)_4]$, $[In(OTf)_3]$, and $[Nd(OTf)_3]$ (10 mol %) were used as the catalysts in DCE, **3a** was produced in 88–94 % total yield and in diastereoselectivities of 7.7:1.0 to 8.2:1.0, but almost no reaction occurred in the presence of $[Yb(OTf)_3]$ (10 mol %) under identical conditions (Table 1, entries 5–9). Use of the Brønsted acid trifluoromethanesulfonic acid (TfOH) led to the formation of **3a** in 92 % total yield under the standard conditions (Table 1, entry 10).

Table 1. Optimization of the reaction conditions.[a]

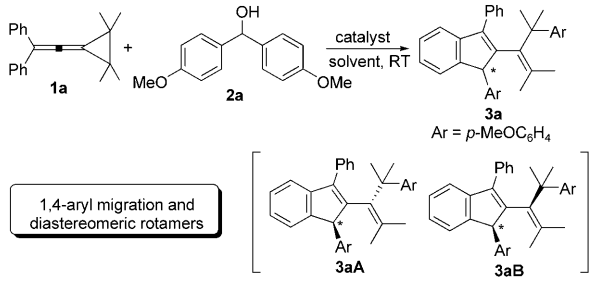

	Catalyst	Solvent	Yield of **3a** [%][b] (ratio **3aA**/**3aB**)
1	$BF_3{\cdot}OEt_2$	CH_2Cl_2	73 (8.1:1.0)
2	$BF_3{\cdot}OEt_2$	CH_3CN	78 (7.9:1.0)
3	$BF_3{\cdot}OEt_2$	toluene	53 (8.2:1.0)
4	$BF_3{\cdot}OEt_2$	DCE	96 (8.3:1.0)
5	$[Sc(OTf)_3]$	DCE	88 (8.0:1.0)
6	$[Zr(OTf)_4]$	DCE	94 (7.7:1.0)
7	$[Yb(OTf)_3]$	DCE	trace[c]
8	$[In(OTf)_3]$	DCE	91 (8.1:1.0)
9	$[Nd(OTf)_3]$	DCE	92 (8.2:1.0)
10	TfOH	DCE	92 (8.0:1.0)

[a] Reaction conditions: **1a** (0.20 mmol), **2a** (0.24 mmol, 1.2 equiv), catalyst (10 mol %), solvent (2.0 mL), RT (20 °C), 5 min (unless specified otherwise). [b] Isolated yield. [c] The reaction mixtures were stirred for 12 h.

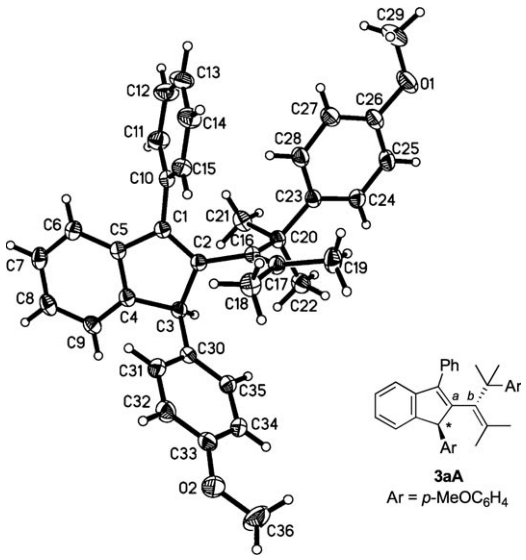

Figure 1. ORTEP drawing of **3aA**.

We also examined the effect of the temperature on this reaction under the tentatively defined optimal conditions, and the results are outlined in Table 2. Reaction temperatures between −10 °C and 50 °C did not significantly affect the reaction outcomes. Therefore, the best reaction conditions were determined to consist of the use of the solvent DCE (2.0 mL) at room temperature (20 °C), VDCPs **1** (0.20 mmol) and bis(aryl)methanols **2** (0.24 mmol, 1.2 equiv) as the substrates, and $BF_3{\cdot}OEt_2$ (10 mol %) as the catalyst. Under these optimal conditions, the reaction went to com-

Table 2. Examination of the effect of the temperature under the standard conditions.[a]

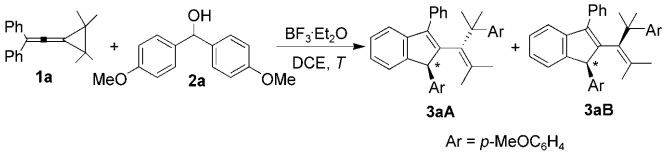

	T	Yield of **3a** [%][b]	Ratio **3aA**/**3aB**[c]
1	−10 °C	97	10.0:1.0
2	RT	96	8.3:1.0
3	50 °C	99	9.1:1.0

[a] Reaction conditions: **1a** (0.20 mmol), **2a** (0.24 mmol, 1.2 equiv), $BF_3{\cdot}OEt_2$ (10 mol%), DCE (2.0 mL). [b] Total isolated yield of **3aA** and **3aB**. [c] Ratio determined from ^{1}H NMR spectroscopic data.

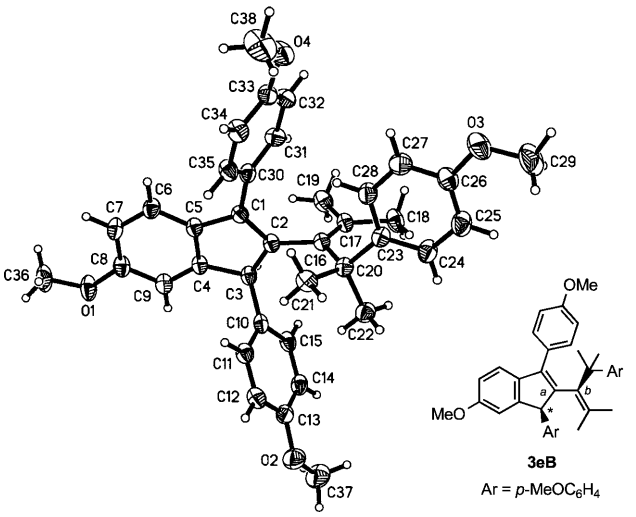

Figure 2. ORTEP drawing of **3eB**.

pletion within 5 minutes, to afford the corresponding adducts **3** in excellent yield.

$BF_3{\cdot}OEt_2$-catalyzed reactions of VDCPs 1b–k with bis(*p*-methoxyphenyl)methanol 2a: With the standard reaction conditions in hand, we next investigated the scope and limitations of this reaction by using a variety of VDCPs **1b–k** with **2a**. The results of these experiments are summarized in Table 3. As can be seen from Table 3, all of these VDCPs **1** reacted smoothly with **2a** to give the corresponding reaction products **3** in excellent yields, regardless of whether they have electron-rich or electron-deficient substituents on the aromatic rings. Furthermore, the structure of another minor diastereomeric rotamer was unambiguously determined by the X-ray diffraction of **3eB** (Figure 2; CIF data presented in the Supporting Information).[11] The two diastereomeric rotamers have the same molecular structure, but have different spatial configurations, because free rotation around the C_a–C_b bond is blocked by steric hindrance between the aryldimethylmethyl group and the two aromatic rings in the product.

When the two aromatic rings are identical (R^1=H, R^2=R^3), a pair of diastereomeric rotamers was obtained in 99% yield (Table 3, entries 1–4). However, if the two aromatic rings are not identical (R^1=H and $R^2 \neq R^3$ or $R^1 \neq$H), the situation is more complicated (Table 3, entries 5–10). Regioisomers can form in addition to their corresponding diastereomeric ro-

Table 3. Reactions of VDCPs **1b–k** with **2a** under the optimal reaction conditions.[a]

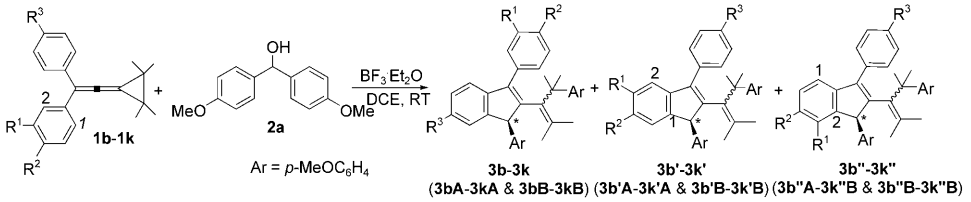

	1 $R^1/R^2/R^3$	Products **3**	Total yield of **3** [%][b] (Ratio **A**/**B**)[c]	Major rotamer **A**[d] ratio **3**/**3′**/**3″**	Minor rotamer **B**[d] ratio **3**/**3′**/**3″**
1	**1b** H/F/F	**3b** (**3bA**, **3bB**)	99 (4.5:1.0)	–	–
2	**1c** H/Cl/Cl	**3c** (**3cA**, **3cB**)	99 (5.1:1.0)	–	–
3	**1d** H/Me/Me	**3d** (**3dA**, **3dB**)	99 (4.9:1.0)	–	–
4	**1e** H/OMe/OMe	**3e** (**3eA**, **3eB**)	99 (3.8:1.0)	–	–
5	**1f** H/H/F	**3f** (**3fA**, **3fB**) **3f′** (**3f′A**, **3f′B**)	97 (7.1:1.0)	1.0:1.0	1.6:1.0
6	**1g** H/H/Cl	**3g** (**3gA**, **3gB**) **3g′** (**3g′A**, **3g′B**)	95 (6.0:1.0)	1.0:1.0	2.1:1.0
7	**1h** H/H/OMe	**3h** (**3hA**, **3hB**) **3h′** (**3h′A**, **3h′B**)	95 (5.2:1.0)	1.5:1.0	3.3:1.0
8	**1i** F/F/H	**3i** (**3iA**, **3iB**) **3i′** (**3i′A**, **3i′B**) **3i′** (**3i′A**, **3i′B**)	99 (5.7:1.0)	8.0:1.0[e]	6.2:1.0[e]
9	**1j** Cl/Cl/H	**3j** (**3jA**, **3jB**) **3j′** (**3j′A**, **3j′B**) **3j′** (**3j′A**, **3j′B**)	90 (6.2:1.0)	12.0:4.0:1.0	10.0:2.9:1.0
10	**1k** Me/Me/H	**3k** (**3kA**, **3kB**) **3k′** (**3k′A**, **3k′B**) **3k′** (**3k′A**, **3k′B**)	97 (4.9:1.0)	3.8:1.0[e]	5.1:1.0[e]

[a] Reaction conditions: **1** (0.20 mmol), **2a** (0.24 mmol, 1.2 equiv), $BF_3{\cdot}OEt_2$ (10 mol%), DCE (2.0 mL), RT, 5 min. [b] Isolated yield. [c] The ratio of the two diastereomeric rotamers. [d] The ratio of the regioisomers in separated major diastereomeric or minor diastereomeric rotamers. [e] The ratio **3i**/**3i′** or **3i**/**3i″** as well as **3k**/**3k′** or **3k**/**3k″** (one of the regioisomers could not be found in the ^{1}H NMR spectra).

tamers; these form in different regioselectivities according to the electronic nature of the aromatic rings—the intramolecular Friedel–Crafts reaction can take place at different aromatic rings (taking place more easily at electron-rich aromatic rings), as well as at different sites of the aromatic rings (Table 3, entries 5–10). The regioselectivities and diastereoselectivities were determined on the basis of NMR spectroscopic data (presented in Supporting Information).

BF_3·OEt_2-catalyzed reactions of VDCP 1a with bis(aryl)methanols 2b–e: We further examined the reaction of VDCP **1a** with a variety of bis(aryl)methanols **2** under the standard reaction conditions (Table 4), and found a distinct effect of the electronic nature of the aromatic rings of **2** on the final reaction outcomes. Electron-rich bis(*p*-alkoxyaryl)methanols **2b** and **2c**, bearing an ethoxy group and an allyloxy group on the phenyl ring, gave the corresponding diastereomeric rotamers **4a** and **4b** in excellent yields by a similar cationic 1,4-aryl-migration process (Table 4, entries 1 and 2). Electron-neutral bis(phenyl)methanol **2d** as the electrophile in the reaction with **1a** under the standard conditions produced the corresponding aryl-migration product **4c** in 58% total yield, after a significantly prolonged reaction time, along with a trialkene product **5a**, resulting from simple proton elimination (Table 4, entry 3). This showed us that the influence of the electronic properties of the aryl rings of the bis(aryl)methanols **2** on the reaction outcome need to be examined. Consequently, it was found that when the electron-deficient bis(*p*-chlorophenyl)methanol (**2e**) was applied in the reaction under the optimal reaction conditions, the reaction became sluggish, affording the corresponding product **5b** exclusively in 91% yield after a week (Table 3, entry 4). We assumed that this is because an electron-rich aromatic ring favors cationic aryl migration and an electron-poor aromatic ring disfavors such a cationic aryl-migration process.[12]

Table 4. Reactions of **1a** with bis(aryl)methanols **2** under the optimal reaction conditions.[a]

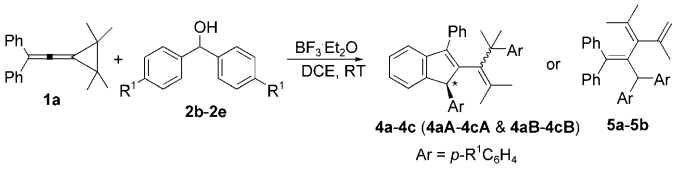

	R^1	Reaction time	Yield [%][b] **4** (ratio **4A**/**4B**)	**5**
1	**2b**: OEt	5 min	**4aA**, **4aB**: 97 (8.1:1.0)	–
2	**2c**: $OCH_2CH{=}CH_2$	5 min	**4bA**, **4bB**: 98 (7.8:1.0)	–
3	**2d**: H	72 h	**4cA**, **4cB**: 58[c]	**5a**: 33
4	**2e**: Cl	1 week	–	**5b**: 91

[a] Reaction conditions: **1a** (0.20 mmol), **2** (0.24 mmol, 1.2 equiv), BF_3·OEt_2 (10 mol%), DCE (2.0 mL), RT (unless specified otherwise). [b] Isolated yields. [c] Only one rotamer was obtained.

BF_3·OEt_2-catalyzed reactions of VDCPs 1l–q with bis(aryl)methanols 2: VDCPs **1l–q**, containing two aromatic groups on the cyclopropane, were also examined in this reaction under the standard reaction conditions, and we found that, apart from the similar 1,4-aryl-migration products, a new set of products was obtained by a different reaction pathway. The results are outlined in Table 5. The reactions with electron-rich bis(*p*-methoxyphenyl)methanol **2a** gave the corresponding product mixtures of diastereomeric rotamers **6** as the major products in good yields by a similar cationic 1,4-aryl-migration process along with the minor products **7** derived from a direct intramolecular Friedel–Crafts reaction (Table 5, entries 1–6). The structure of the major rotamer of **6a**, obtained from the product mixtures of the diastereomeric rotamers **6a** formed by the reaction of **1l** with **2a**, as well as the structure of the minor product **7e** formed in the reaction of **1p** with **2a** were determined by X-ray diffraction (Figures 3 and 4; CIF data in Supporting Information).[13,14]

The use of electron-neutral bis(phenyl)methanol (**2d**), electron-deficient bis(*p*-chlorophenyl)methanol (**2e**), or less-electron-rich bis(*p*-methylphenyl)methanol (**2f**) as the electrophiles to react with VDCP **1l** under the standard conditions afforded the corresponding products **7g–i** exclusively in >99% yields (Table 5, entries 7–9). As mentioned above, the electron-rich aromatic ring in **2** favors cationic 1,4-aryl

Table 5. Reactions of VDCPs **1l–q** with bis(aryl)methanols **2** under the optimal reaction conditions.[a]

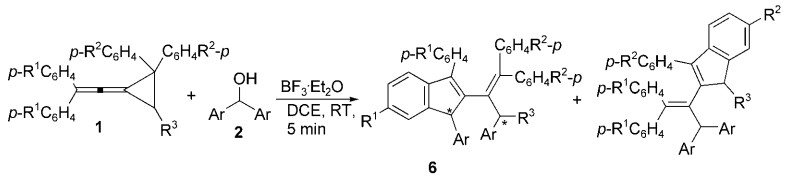

	1	R^1	R^2	R^3	**2**	Ar	Yield of **6** [%][b,c]	Yield of **7** [%][b]
1	**1l**	H	H	Me	**2a**	p-$MeOC_6H_4$	**6a**: 88 (26.0:9.7:4.7:1.0)	**7a**: 11
2	**1m**	H	H	Et	**2a**	p-$MeOC_6H_4$	**6b**: 84 (46.2:33.8:5.3:1.0)	**7b**: 15
3	**1n**	Me	H	Me	**2a**	p-$MeOC_6H_4$	**6c**: 81 (30.0:9.0:4.0:1.0)	**7c**: 17
4	**1o**	Cl	H	Me	**2a**	p-$MeOC_6H_4$	**6d**: 88 (35.8:12.1:3.8:1.0)	**7d**: 11
5	**1p**	H	Me	Me	**2a**	p-$MeOC_6H_4$	**6e**: 85 (10.0:4.8:1.0:–)	**7e**: 13
6	**1q**	H	Cl	Me	**2a**	p-$MeOC_6H_4$	**6f**: 79 (9.6:3.5:1.0:–)	**7f**: 19
7	**1l**	H	H	Me	**2d**	C_6H_5	–	**7g**: >99
8	**1l**	H	H	Me	**2e**	p-ClC_6H_4	–	**7h**: >99
9	**1l**	H	H	Me	**2f**	p-MeC_6H_4	–	**7i**: >99

[a] Reaction conditions: VDCP **1** (0.20 mmol), bis(aryl)methanol **2** (0.24 mmol, 1.2 equiv), BF_3·OEt_2 (10 mol%), DCE (2.0 mL), RT, several minutes (unless specified otherwise). [b] Total isolated yield. [c] The values in parentheses are the ratios of the diastereomeric rotamers, determined from ^1H NMR spectroscopic data.

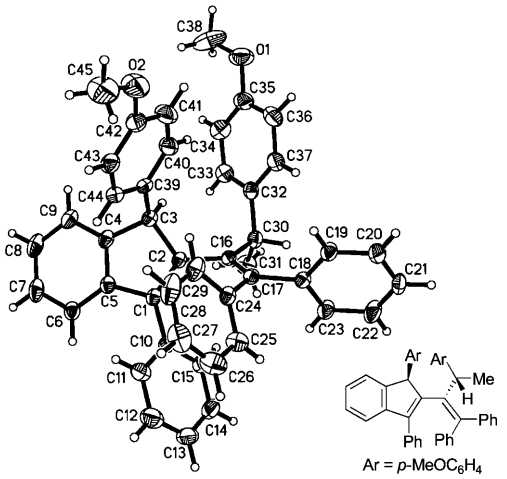

Figure 3. ORTEP drawing of the major rotamer of **6a**.

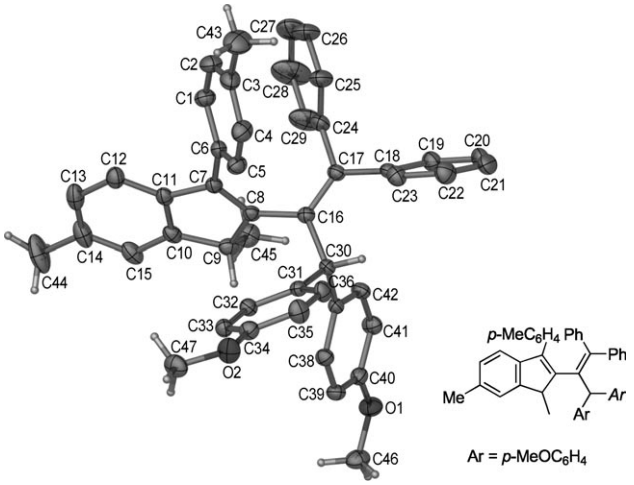

Figure 4. ORTEP drawing of **7e**.

migration. However, in this case, the $BF_3{\cdot}OEt_2$-catalyzed intramolecular Friedel–Crafts reaction of the carbocation derived from the ring opening of cyclopropane with the aromatic ring at the cyclopropane takes place easily to give the corresponding products **7**. This reaction pathway became dominant when less-electron-rich bis(aryl)methanols **2** were used as the electrophiles (Table 5, entries 7–9). It should be noted that, because product **6** has two chiral centers, four diastereomeric rotamers could be formed, as shown in Table 5, and their ratios were determined from the NMR spectroscopic data (Figure 5). The stereochemistry of the major diastereomeric rotamer was determined by X-ray crystallography.

Theoretical study: To understand the mechanism of this reaction, DFT[15] studies were performed by use of the GAUSSIAN03 program[16] using the B3LYP[17] method and the 6-31+G** basis set. In the study of the reaction pathways, the solvent effect was estimated with IEFPCM[18] (UAHF atomic radii) method (DCE, $\varepsilon = 10.36$) on the basis of the

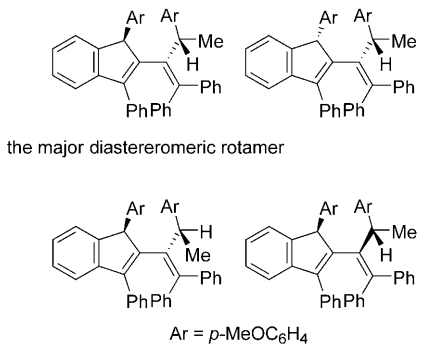

Figure 5. Four diastereomeric rotamers in the formation of **6**.

gas-phase fully optimized structures. For each structure, harmonic vibration frequency calculations were carried out and thermal corrections were made. All structures were shown as the transition states (with one imaginary frequency) or the stationary points (with no imaginary frequency).

The rotation barrier between 3aA and 3aB: Simplified models **3aA′** and **3aB′** without the OMe groups were used for calculating the rotation barrier between **3aA** and **3aB** (Figure 6). On the basis of a relaxed potential energy surface (PES) scan on the B3LYP/6-31G* level along the dihedral angle D_{1234} (see Supporting Information SI-Figure 1), the rotational transition state **TS-rotation** was located. Then, **3aA′**, **3aB′**, and **TS-rotation** were reoptimized at the B3LYP/6-31+G** level (Figure 6). The rotational barrier is quite high (up to 36.2 kcal mol^{-1}), suggesting that rotamers **3aA** and **3aB** cannot isomerize into one another at room temperature or even upon heating. This phenomenon was identified by our experimental results, because we found that heating **3aB** in refluxing toluene only resulted in decomposition of the product mixtures without formation of **3aA**. Rotamer **3aA′** is 1.0 kcal mol^{-1} more stable than **3aB′**. The relative stabilities of **3aA** and **3aB** are depicted qualitatively by the illustrations shown in Figure 6. In **3aA**, the 1-aryl group is adjacent to the smaller G1 group, whereas in **3aB**, it is adjacent to the larger G2 group, consequently leading to larger steric repulsion and higher energy. The congested structure of **3aB** is also disfavored in terms of entropy.

The reaction pathways: We started the calculation with the allylic cationic intermediate **D** (Scheme 2). All of the optimized structures are collected in the Supporting Information, and some selected structures are shown in Figure 7. In intermediate **D**, Ph1 is parallel to the plane of the allylic cation, and Ph2 is far from the two Ar groups, thus avoiding steric repulsion. Theoretical studies suggest that aryl migrations from I to O[19a,b] and alkyl-group migrations from Cl to O[19c] are by concerted one-step mechanisms without any intermediates. However, our calculations indicate that the 1,4-aryl migration from C1 to C4 is a two-step process. In **TS-DE**, one of the aryl groups is migrating from C1 to C4, leading to the spirocyclopentylbenzenium intermediate **E**

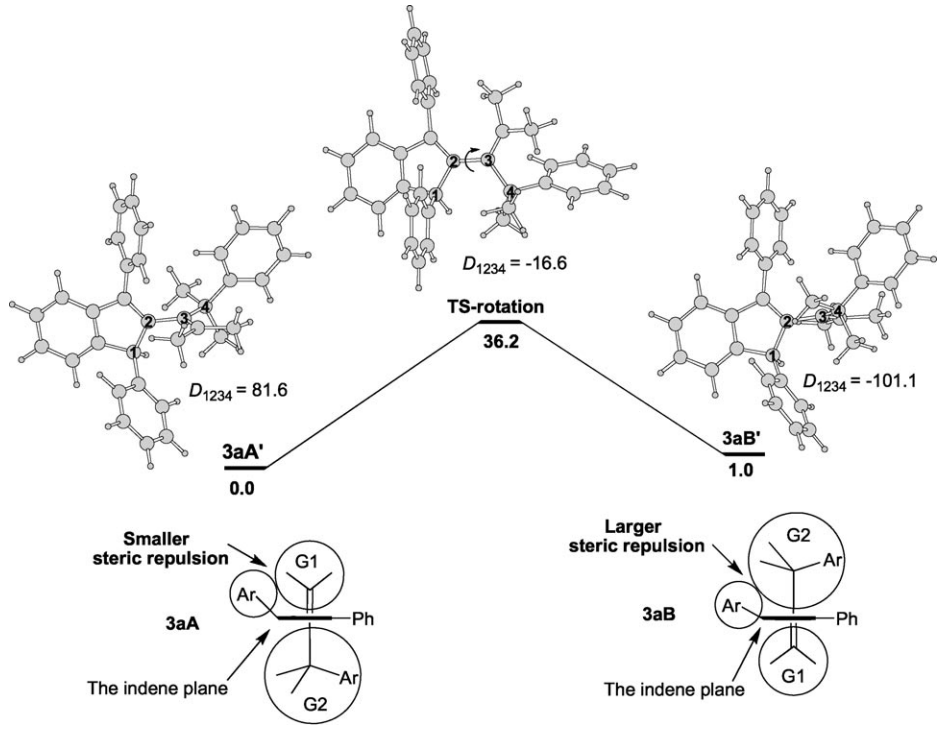

Figure 6. The optimized structures of **3aA′**, **3aB′**, **TS-rotation** and graphics to help understand the relative stabilities of **3aA** and **3aB**. The relative free energies in the gas phase [ΔG_{gas} (298 K), kcal mol^{-1}] and the dihedral angles [D, °] are provided. The geometries were fully optimized at the B3LYP/6-31+G** level.

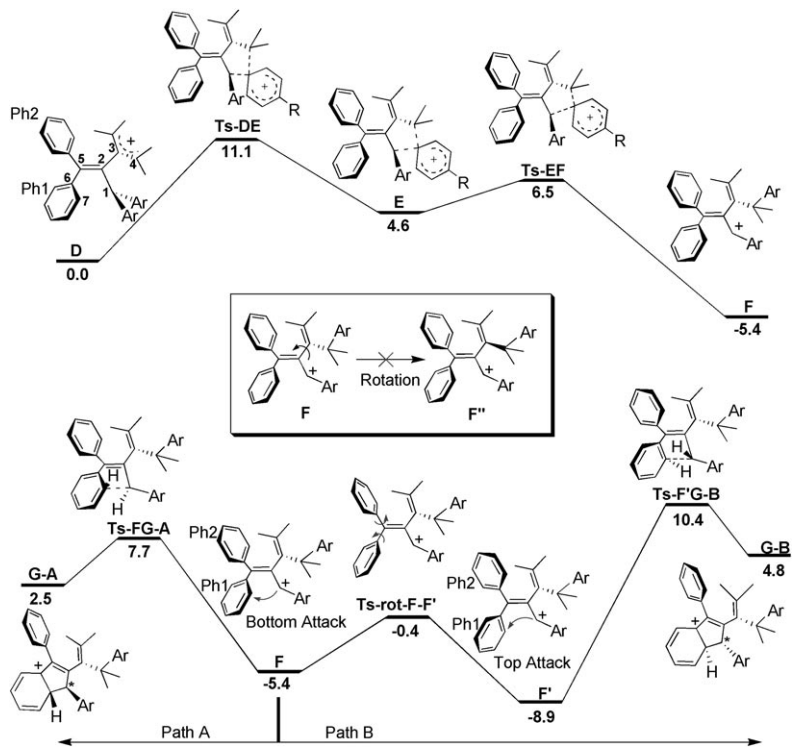

Scheme 2. Reaction pathways and the relative free energies including solvent effect ΔG_{sol} [kcal mol^{-1}, 298 K]. These were calculated on the B3LYP/6-31+G** level.

(Scheme 2). Then, intermediate **E** transforms into the allylic cation **F** via transition state **TS-EF** over a small barrier of 1.9 kcal mol^{-1}. The two transition states **TS-DE** and **TS-EF** and intermediate **E** all have five-membered-ring structures. In intermediate **D**, the net Mulliken charge of the methoxy group in the leaving aryl group is +0.016, and the C–O distance is 1.353 Å. In contrast, in the phenonium intermediate **E**, the net Mulliken charge of the methoxy group increases to +0.096, and the C–O distance decreases to 1.315 Å. Similar changes can also be found in the two transition states **TS-DE** and **TS-EF**. These results indicate that the *p*-methoxy group has a great effect on the stabilization of the phenonium intermediate and the transition states involved, as proposed by Tahir Khan et al.[9a]

Along path A, the carbocation attacks Ph1 from below. Intermediate **F** undergoes an intramolecular Friedel–Crafts reaction to form intermediate **G-A** via **TS-FG-A**; **G-A** is then transformed into the final major product **3aA** after deprotonation. As mentioned above, the products **3aA** and **3aB** cannot transform into one another by rotation around the C2–C3 bond at room temperature. A relaxed potential energy surface scan shows that intermediate **F** also cannot transform into **F″** by rotation around the C2–C3 bond, which leads to **3aB**. On the basis of another relaxed potential energy surface scan, the rotational transition state **TS-Rot-F-F′** was located. In this transition state, the orientation of Ph1 and Ph2 flips over at the same time. Thus, along path B, **F** can transform into **F′** over a small barrier of 5.0 kcal mol^{-1}. Then the carbocation attacks Ph1 from above via **Ts-F′G-B**

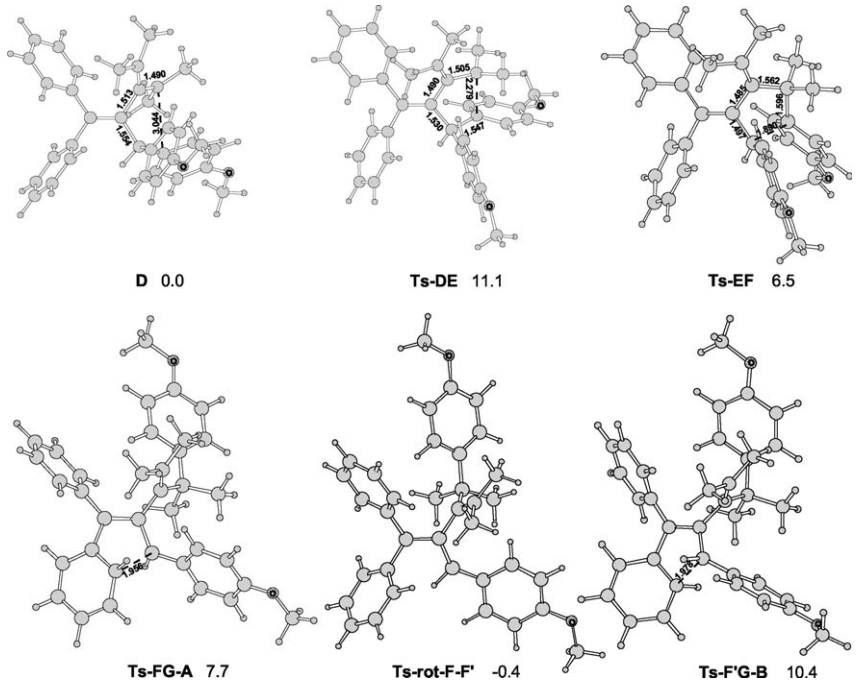

Figure 7. Selected optimized structures along the reaction pathways. Some bond lengths [Å], bond angles [°], and relative free energies including the solvent effect [ΔG_{sol} (298 K), kcal mol^{-1}] are shown. The geometries were fully optimized at the B3LYP/6-31+G** level.

to form intermediate **G-B**, which is then transformed into the final minor product **3aB** after deprotonation.

The preference for the major product **3aA** originates from the relative stabilities of **Ts-FG-A** and **Ts-F′G-B**, which can also be understood qualitatively by the steric effects shown in Figure 7.

On the basis of the above experimental and computational results, a plausible mechanism for the formation of **3**, **4**, and **5** was found, and is outlined in Scheme 3 using **1a** as an example. The reaction is initiated by the generation of the carbocationic intermediate **A** from bis(aryl)methanol **2** in the presence of $BF_3{\cdot}OEt_2$, which attacks the central carbon of the allene moiety of **1a** to produce the cationic intermediate **B**. Intermediate **B** then immediately undergoes ring opening to afford allylic cation **C** or its resonance structure **D**. In intermediate **D**, when the aromatic ring (Ar) has an electron-donating group, the 1,4-aryl migration takes place via the cationic transition state **E** (a five-membered-ring intermediate) to afford another allylic cation **F**, which undergoes intramolecular Friedel–Crafts reaction to furnish the final product **3**. When the aromatic ring (Ar) in intermediate **D** has an electron-withdrawing group, the aromatic ring does not undergo aryl migration, but instead undergoes direct deprotonation to afford product **5**.

In contrast, in the case of VDCPs **1l–q**, the plausible reaction mechanism outlined in Scheme 4, using **1l** as a model, was derived. The reaction undergoes the same process for the formation of the carbocationic intermediate **A**, followed by electrophilic attack and subsequent ring opening of the cyclopropyl cation to produce intermediate **D′**. Two reaction pathways are available for the next steps in this case. In path A, the intramolecular Friedel–Crafts reaction takes place directly to afford the final product **7** via intermediate **G″**. In path B, however, intermediate **D′** undergoes the same 1,4-aryl migration via a five-membered cationic transition state **E′** to furnish intermediate **F′** when the aromatic ring (Ar) has an electron-donating group, and the next intramolecular Friedel–Crafts reaction takes place to produce product **6** via intermediate **G′**. It can be seen that besides the electronic nature of the employed bis(aryl)methanols **2**, the substituents on the cyclopropane of the employed VDCPs **1** can also affect the reaction pathways and the subsequent final reaction outcomes.

Conclusion

The $BF_3{\cdot}OEt_2$-catalyzed reactions of VDCPs **1** with bis(aryl)methanols **2** under mild conditions were examined. Depending on the electronic nature of the employed bis(aryl)methanols and the substituents on the cyclopropane of the VDCPs, the reaction underwent different pathways to afford three kinds of products. From electron-rich bis(aryl)methanols **2a–c**, indene derivatives **3**, **4**, and **6** were

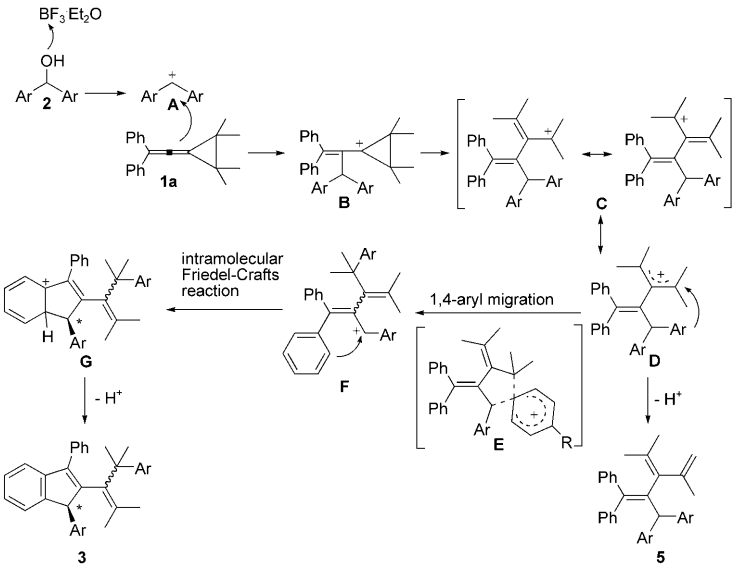

Scheme 3. A plausible reaction mechanism of VDCPs **1a–k** with bis(aryl)methanols **2**.

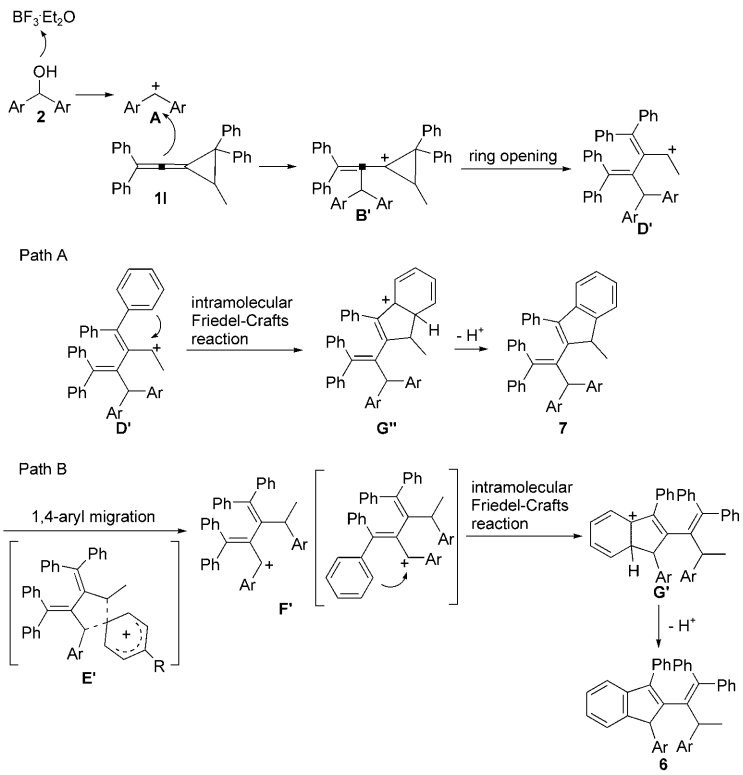

Scheme 4. A plausible reaction mechanism of VDCPs **1l–q** with bis(aryl)methanols **2**.

obtained in good to excellent yields as mixtures of diastereomeric rotamers by a novel cationic 1,4-aryl migration between carbon atoms and a subsequent intramolecular Friedel–Crafts reaction. On the other hand, in the case of electron-deficient, electron-neutral, or less-electron-rich bis(aryl)methanols **2d–f**, other reaction processes took place rather than the aryl migration, and the corresponding trialkene compounds **5**, derived from direct deprotonation, as well as another kind of indene derivatives **7**, derived from direct intramolecular Friedel–Crafts reaction, were produced in moderate to excellent yields. On the basis of the experimental results in conjunction with further computational studies, plausible mechanisms for all these reactions were proposed. Efforts are in progress to elucidate further mechanistic details of these reactions and to understand their scope and limitations.

Experimental Section

General: ^{1}H and ^{13}C NMR spectra were recorded at 300 (or 400) and 75 (or 100) MHz, respectively. MS and HRMS were carried out by the EI method. Organic solvents that were used were dried by standard methods when necessary. Satisfactory CHN microanalyses were obtained with an analyzer. Commercially obtained reagents were used without further purification. All these reactions were monitored by TLC (silica gel coated plates). Flash column chromatography was carried out on silica gel at increased pressure.

General procedure for $BF_3{\cdot}OEt_2$-catalyzed reactions of VDCPs 1 with bis(aryl)methanols 2: Under an argon atmosphere, VDCP **1** (0.20 mmol), bis(aryl)methanol **2** (0.24 mmol, 1.2 equiv), and DCE (2.0 mL) were loaded into a Schlenk tube. The reaction mixture was stirred at RT (20 °C), and then $BF_3{\cdot}OEt_2$ (10 mol%) was added. After 5 min, the solvent was removed under reduced pressure and the residue was purified by flash column chromatography.

Compound 3aA: White solid; m.p. 194–197 °C; ^{1}H NMR (300 MHz, $CDCl_3$): δ = 0.91 (s, 3H; CH_3), 0.98 (s, 3H; CH_3), 1.00 (s, 3H; CH_3), 1.64 (s, 3H; CH_3), 3.71 (s, 3H; CH_3), 3.78 (s, 3H; CH_3), 4.74 (s, 1H; CH), 6.52 (d, , J = 9.0 Hz, 2H; Ar), 6.67 (d, J = 9.0 Hz, 2H; Ar), 6.77 (d, J = 9.0 Hz, 2H; Ar), 7.00 (d, J = 9.0 Hz, 2H; Ar), 7.20–7.25 (m, 1H; Ar), 7.31–7.33 (m, 3H; Ar), 7.40–7.49 ppm (m, 5H; Ar); ^{13}C NMR (75 MHz, $CDCl_3$): δ = 21.3, 25.6, 28.6, 33.1, 43.4, 55.0, 55.2, 59.9, 112.9, 113.3, 120.0, 124.5, 125.1, 126.8, 127.3, 128.4, 129.1, 130.6, 131.5, 134.0, 134.3, 136.3, 138.6, 144.6, 145.8, 147.3, 149.9, 156.6, 158.4 ppm; IR (CH_2Cl_2): $\tilde{\nu}$ = 2961, 2930, 2906, 2835, 1608, 1509, 1463, 1442, 1374, 1299, 1249, 1179, 1036, 830, 785, 740, 702, 656 cm^{-1}; MS (EI): m/z (%): 500 (9) $[M]^+$, 352 (30), 351 (92), 244 (21), 243 (100), 228 (13), 149 (78), 121 (28), 91 (9), 41 (10); elemental analysis calcd (%) for $C_{36}H_{36}O_2$: C 86.36, H 7.25; found: C, 86.41, H 7.32.

Compound 3aB: White solid; m.p. 190–195 °C; ^{1}H NMR (300 MHz, $CDCl_3$): δ = 0.60 (s, 3H; CH_3), 0.74 (s, 3H; CH_3), 1.18 (s, 3H; CH_3), 1.87 (s, 3H; CH_3), 3.69 (s, 3H; CH_3), 3.81 (s, 3H; CH_3), 4.82 (s, 1H; CH), 6.44 (d, J = 9.0 Hz, 2H; Ar), 6.51 (d, J = 9.0 Hz, 2H; Ar), 6.84–6.87 (m, 2H; Ar), 7.15–7.28 (m, 5H; Ar), 7.39–7.52 ppm (m, 5H; Ar); IR (CH_2Cl_2): $\tilde{\nu}$ = 2932, 2906, 2834, 1733, 1609, 1510, 1463, 1248, 1179, 1036, 830, 760, 702 cm^{-1}; MS (EI): m/z (%): 500 (7) $[M]^+$, 351 (100), 321 (10), 273 (12), 243 (85), 149 (73), 121 (25), 85 (20), 71 (22), 57 (30), 43 (20), 41 (17); HRMS (EI): m/z: calcd for $C_{36}H_{36}O_2$: 500.2715; found: 500.2718.

Compound 5a: Colorless liquid; ^{1}H NMR (300 MHz, $CDCl_3$): δ = 1.08 (s, 3H; CH_3), 1.41 (s, 3H; CH_3), 1.46 (s, 3H; CH_3), 4.43 (d, J = 2.1 Hz, 1H; CH_2 =), 4.74 (d, J = 2.1 Hz, 1H; CH_2 =), 5.39 (s, 1H; CH), 7.08–7.26 ppm (m, 20H; Ar); ^{13}C NMR (75 MHz, $CDCl_3$): δ = 21.4, 23.2, 23.8, 55.7, 116.9, 125.6, 126.0, 126.4, 127.2, 127.6, 128.2, 128.8, 129.0, 129.3, 130.7, 133.6, 133.9, 139.1, 141.9, 142.5, 143.1, 143.3, 143.7, 145.6 ppm; IR (CH_2Cl_2): $\tilde{\nu}$ = 3057, 3025, 2923, 2852, 1797, 1598, 1493, 1443, 1075, 898, 743, 698, 586 cm^{-1}; MS (EI): m/z (%): 440 (100) $[M]^+$, 349 (11), 321 (26), 291 (19), 273 (44), 243 (32), 207 (21), 167 (60), 91 (16); HRMS (EI): m/z: calcd for $C_{34}H_{32}$: 440.2504; found: 440.2504.

Compound 7a: White solid; m.p. 247–250 °C; ^{1}H NMR (300 MHz, $CDCl_3$): δ = 1.10 (d, J = 7.5 Hz, 3H; CH_3), 3.56 (q, J = 7.5 Hz, 1H; CH), 3.76 (s, 3H; CH_3), 3.82 (s, 3H; CH_3), 5.53 (s, 1H; CH), 6.35 (d, J = 6.9 Hz, 2H; Ar), 6.39 (d, J = 7.5 Hz, 2H; Ar), 6.75–6.87 (m, 7H; Ar), 6.94 (d, J = 8.4 Hz, 2H; Ar), 7.02–7.41 ppm (m, 14H; Ar); ^{13}C NMR (75 MHz, $CDCl_3$): δ = 17.4, 47.1, 53.2, 55.2, 55.3, 113.4, 114.1, 120.4, 122.5, 124.7, 125.6, 126.1, 126.4, 126.8, 127.0, 127.7, 128.3, 128.5, 129.0, 129.4, 129.7, 131.2, 132.1, 135.0, 135.5, 142.2, 142.8, 143.5, 143.7, 144.0, 147.2, 149.0, 158.0, 158.2 ppm; IR (CH_2Cl_2): $\tilde{\nu}$ = 3055, 2955, 2927, 1608, 1509, 1462, 1249, 1178, 1034, 747, 699 cm^{-1}; MS (EI): m/z (%): 610 (8) $[M]^+$, 383 (10), 367 (5), 305 (9), 291 (10), 227 (100), 167 (4), 91 (2); ; HRMS (EI): m/z: calcd for $C_{45}H_{38}O_2$: 610.2872; found: 610.2873.

Compound 6a: Contains a trace of diastereomeric isomers; white solid; m.p. 216–218 °C; ^{1}H NMR (300 MHz, $CDCl_3$): δ = 1.48 (d, J = 7.5 Hz, 3H; CH_3), 3.76 (s, 3H; CH_3), 3.86 (s, 3H; CH_3), 4.44 (q, J = 7.5 Hz, 1H; CH), 4.52 (s, 1H; CH), 5.89 (d, J = 8.1 Hz, 2H; Ar), 6.04 (d, J = 8.1 Hz, 2H; Ar), 6.25–6.40 (m, 1H; Ar), 6.56 (d, J = 8.4 Hz, 2H; Ar), 6.73 (t, J = 7.8 Hz, 2H; Ar), 6.89 (d, J = 8.4 Hz, 2H; Ar), 6.90–7.78 ppm (m, 16H; Ar); ^{13}C NMR (75 MHz, $CDCl_3$): δ = 17.0, 39.9, 55.1, 55.4, 57.1, 112.6, 114.0, 120.0, 123.9, 125.3, 125.7, 126.2, 126.4, 126.7, 128.0, 128.2, 128.87, 129.1, 129.4, 129.6, 130.7, 130.9, 135.5, 136.2, 136.4, 142.76, 142.83, 142.9, 144.2, 146.8, 149.5, 158.0, 158.3 ppm; IR (CH_2Cl_2): $\tilde{\nu}$ = 3055, 2955, 2928, 1608, 1509, 1490, 1462, 1302, 1249, 1178, 1036, 830, 743, 702, 572, 535 cm^{-1}; ; MS (EI): m/z (%): 500 (9) $[M]^+$, 352 (30), 351 (92), 244 (21), 243 (100), 228 (13), 149 (78), 121 (28), 91 (9), 41 (10); elemental analysis calcd (%) for $C_{45}H_{38}O_2$: C 88.49, H 6.27; found: C 88.40, H 6.21.

Acknowledgements

We thank the Shanghai Municipal Committee of Science and Technology (06XD14005, 08dj1400100-2), the National Basic Research Program of China (973-2009CB825300), and the National Natural Science Foundation of China (20872162, 20672127, 20821002, 20732008, 20702059) for financial support, and also thank Mr. Sun Jie for performing the X-ray diffraction.

[1] For the synthesis of VDCPs, see: a) K. Isagawa, K. Mizuno, H. Sugita, Y. Otsuji, *J. Chem. Soc. Perkin Trans. 1* **1991**, 2283–2285, and references therein; b) T. Sasaki, S. Eguchi, M. Ohno, F. Nakata, *J. Org. Chem.* **1976**, *41*, 2408–2411; c) T. Sasaki, S. Eguchi, T. Ogawa, *J. Org. Chem.* **1974**, *39*, 1927–1930; d) T. Sasaki, S. Eguchi, T. Ogawa, *Heterocycles* **1975**, *3*, 193–196; e) S. Eguchi, M. Arasaki, *J. Chem. Soc. Perkin Trans. 1* **1988**, 1047–1050; f) H. Sugita, K. Mizuno, T. Mori, K. Isagawa, Y. Otsuji, *Angew. Chem.* **1991**, *103*, 1000–1002; *Angew. Chem. Int. Ed. Engl.* **1991**, *30*, 984–986; g) T. B. Patrick, *Tetrahedron Lett.* **1974**, *15*, 1407–1408; h) J. R. Al Dulayymi, M. S. Baird, *J. Chem. Soc. Perkin Trans. 1* **1994**, 1547–1548; i) T. B. Patrick, *J. Org. Chem.* **1977**, *42*, 3354–3356; j) H. D. Hartzler, *J. Am. Chem. Soc.* **1971**, *93*, 4527–4531; k) H. Maeda, K. Mizuno, *J. Synth. Org. Chem. Jpn.* **2004**, *62*, 1014–1025.

[2] a) K. Mizuno, H. Sugita, T. Hirai, H. Maeda, Y. Otsuji, M. Yasuda, M. Hashiguchi, K. Shima, *Tetrahedron Lett.* **2001**, *42*, 3363–3366; b) K. Mizuno, K. Nire, H. Sugita, Y. Otsuji, *Tetrahedron Lett.* **1993**, *34*, 6563–6566; c) T. Sasaki, S. Eguchi, T. Ogawa, *J. Am. Chem. Soc.* **1975**, *97*, 4413–4414.

[3] a) W. Li, M. Shi, *J. Org. Chem.* **2008**, *73*, 4151–4154; b) J.-M. Lu, M. Shi, *Tetrahedron* **2006**, *62*, 9115–9122; c) Y. Fall, H. Doucet, M. Santelli, *Tetrahedron Lett.* **2007**, *48*, 3579–3581; d) J.-M. Lu, M. Shi, *Tetrahedron* **2007**, *63*, 7545–7549; e) Y.-P. Zhang, J.-M. Lu, G.-X. Xu, M. Shi, *J. Org. Chem.* **2007**, *72*, 509–516; f) L.-X. Shao, Y.-P. Zhang, M.-H. Qi, M. Shi, *Org. Lett.* **2007**, *9*, 117–120; g) G.-C. Xu, L.-P. Liu, J.-M. Lu, M. Shi, *J. Am. Chem. Soc.* **2005**, *127*, 14552–14553; h) G.-C. Xu, M. Ma, L.-P. Liu, M. Shi, *Synlett* **2005**, 1869–1872; i) J.-M. Lu, M. Shi, *Org. Lett.* **2006**, *8*, 5317–5320; j) J.-M. Lu, M. Shi, *Org. Lett.* **2007**, *9*, 1805–1808; k) Z.-B. Zhu, L.-X. Shao, M. Shi, *Eur. J. Org. Chem.* **2009**, 2576–2580; l) F.-F. Yu, W.-G. Yang, M. Shi, *Chem. Commun.* **2009**, 1392–1394; m) C.-L. Su, X. Huang, Q.-Y. Liu, X. Huang, *J. Org. Chem.* **2009**, *74*, 8272–8279; n) W. Li, W. Yuan, M. Shi, E. Hernandez, G.-G. Li, *Org. Lett.* **2010**, *12*, 64–67; o) J.-M. Lu, M. Shi, *Org. Lett.* **2008**, *10*, 1943–1946; p) J.-M. Lu, M. Shi, *Chem. Eur. J.* **2009**, *15*, 6065–6073; q) B.-L. Lu, J.-M. Lu, M. Shi, *Tetrahedron* **2009**, *65*, 9328–9335; r) B.-L. Lu, J.-M. Lu, M. Shi, *Tetrahedron Lett.* **2010**, *51*, 321–324.

[4] A. V. Stepakov, A. G. Larina, A. P. Molchanov, L. V. Stepakova, G. L. Starova, R. R. Kostikov, *Russ. J. Org. Chem.* **2007**, *43*, 40–49.

[5] a) L. Wu, J.-M. Lu, M. Shi, *J. Org. Chem.* **2008**, *73*, 8344–8347; b) L. Wu, J.-M. Lu, M. Shi, *Tetrahedron* **2008**, *64*, 3315–3321; c) J.-M. Lu, M. Shi, *J. Org. Chem.* **2008**, *73*, 2206–2210; d) M. Shi, L.-F. Yao, *Chem. Eur. J.* **2008**, *14*, 8725–8731; e) J.-M. Lu, Z.-B. Zhu, M. Shi, *Chem. Eur. J.* **2009**, *15*, 963–971; f) Z.-B. Zhu, M. Shi, *Chem. Eur. J.* **2008**, *14*, 10219–10222; g) M. Shi, W. Li, *Tetrahedron* **2007**, *63*, 6654–6660; h) W. Li, M. Shi, *Tetrahedron* **2007**, *63*, 11016–11020; i) W. Li, M. Shi, *J. Org. Chem.* **2008**, *73*, 6698–6705; j) W. Li, M. Shi, *Eur. J. Org. Chem.* **2009**, 270–274; k) W. Li, M. Shi, *J. Org. Chem.* **2009**, *74*, 856–860; l) L.-F. Yao, M. Shi, *Chem. Eur. J.* **2009**, *15*, 3875–3881; m) W. Li, M. Shi, Y.-X. Li, *Chem. Eur. J.* **2009**, *15*, 8852–8860; for the Lewis acid catalyzed reactions of bis(4-alkoxyphenyl)methanol with (diarylmethylene)- and (dialkylmethylene)cyclopropanes, see: n) L.-F. Yao, M. Shi, *Eur. J. Org. Chem.* **2009**, 4971–4982.

[6] H. Wieland, *Chem. Ber.* **1911**, *44*, 2550–2556.

[7] W. H. Urry, M. S. Kharasch, *J. Am. Chem. Soc.* **1944**, *66*, 1438–1442.

[8] For a review on radical aryl migrations, see: a) A. Studer, M. Bossart, *Tetrahedron* **2001**, *57*, 9649–9667; b) A. Studer, M. Bossart, *Radicals in Organic Synthesis, Vol. 2* (Eds.: P. Renaud, M. P. Sibi), Wiley-VCH, Weinheim, **2001**, pp. 62–76; c) W. S. Trahanovsky, D. E. Zabel, M. L. S. Louie, *J. Org. Chem.* **1973**, *38*, 757–759; d) A. Studer, M. Bossart, T. Vasella, *Org. Lett.* **2000**, *2*, 985–988; e) K. Wakabayashi, H. Yorimitsu, H. Shinokubo, K. Oshima, *Org. Lett.* **2000**, *2*, 1899–1901; f) P. C. Montevecchi, M. L. Navacchia, *J. Org. Chem.* **1997**, *62*, 5600–5607; g) A. Gheorghe, B. Quiclet-Sire, X. Vila, S. Z. Zard, *Org. Lett.* **2005**, *7*, 1653–1656; h) S. Amrein, M. Bossart, T. Vasella, A. Studer, *J. Org. Chem.* **2000**, *65*, 4281–4288.

[9] a) T. Khan, P. J. Skabara, S. J. Coles, M. B. Hursthouse, *Chem. Commun.* **2001**, 369–370; b) J. W. Wilt, T. P. Malloy, P. K. Mookerjee, D. R. Sullivan, *J. Org. Chem.* **1974**, *39*, 1327–1336; c) J. W. Wilt, T. P. Malloy, *J. Am. Chem. Soc.* **1970**, *92*, 4747–4749; d) M. Takahashi, N. Sekine, T. Fujita, S. Watanabe, K. Yamaguchi, M. Sakamoto, *J. Am. Chem. Soc.* **1998**, *120*, 12770–12776; e) K. Tomooka, A. Nakazaki, T. Nakai, *J. Am. Chem. Soc.* **2000**, *122*, 408–409; f) A. Nakazaki, J. Usuki, K. Tomooka, *Synlett* **2008**, 2064–2068; g) O. L. Chapman, T. H. Kinstle, M. T. Sung, *J. Am. Chem. Soc.* **1966**, *88*, 2618–2619. For a few examples of anionic 1,4-aryl migrations, see: h) E. Grovenstein, Jr., J. A. Beres, Y.-R. Cheng, J. Pegolott, *J. Org. Chem.* **1972**, *37*, 1281–1292.

[10] Crystal data of **3aA**: formula: $C_{36}H_{36}O_2$; M_r: 500.65; crystal color, habit: colorless, prismatic; crystal system: triclinic, lattice type: primitive; lattice parameters: $a=10.9712(10)$, $b=11.1396(10)$, $c=12.7340(12)$ Å; $\alpha=84.184(2)$, $\beta=71.499(2)$, $\gamma=74.938(2)°$; $V=1424.8(2)$ Å^3; space group: $P\bar{1}$; $Z=2$; $\rho_{calcd}=1.167$ g cm^{-3}; $F_{000}=536$; diffractometer: Rigaku AFC7R; residuals: R, Rw: 0.0528, 0.1286. CCDC-678274 contains the supplementary crystallographic data for **3aA**. These data can be obtained free of charge from The Cambridge Crystallographic Data Centre via www.ccdc.cam.ac.uk/data_request/cif.

[11] Crystal data of **3eB**: formula: $C_{38}H_{40}O_4$; M_r: 560.70; crystal color, habit: colorless, prismatic; crystal system: monoclinic, lattice type: primitive; lattice parameters: $a=12.3292(13)$, $b=8.2702(9)$, $c=31.355(3)$ Å; $\alpha=90$, $\beta=98.443(2)$, $\gamma=90°$; $V=3162.5(6)$ Å^3; space group: $P2_1/n$; $Z=4$; $\rho_{calcd}=1.178$ g cm^{-3}; $F_{000}=1200$; diffractometer: Rigaku AFC7R; residuals: R, Rw: 0.0625, 0.1397. CCDC-682291 contains the supplementary crystallographic data for **3eB**. These data can be obtained free of charge from The Cambridge Crystallographic Data Centre via www.ccdc.cam.ac.uk/data_request/cif.

[12] a) B. Florian, D. Henri, S. Maurice, *Synthesis* **2005**, 3589–3602; b) J. P. Sajan, D. N. Dhar, *Tetrahedron* **1986**, *42*, 5979–5983; c) K. Hiroyuki, T. Jun, I. Nobuharu, *J. Am. Chem. Soc.* **2002**, *124*, 11592–11593.

[13] Crystal data of **6a**: formula: $C_{45}H_{38}O_2$; M_r: 610.75; crystal color, habit: colorless, prismatic; crystal system: monoclinic; lattice type: primitive; lattice parameters: $a=8.5135(9)$, $b=21.504(2)$, $c=9.8635(10)$ Å; $\alpha=90$, $\beta=110.542(2)$, $\gamma=90°$; $V=1691.0(3)$ Å^3; space group: $P2_1$; $Z=2$; $\rho_{calcd}=1.200$ g cm^{-3}; $F_{000}=648$; diffractometer: Rigaku AFC7R; residuals: R, Rw: 0.0449, 0.0815. CCDC-686803 contains the supplementary crystallographic data for **6a**. These data can be obtained free of charge from The Cambridge Crystallographic Data Centre via www.ccdc.cam.ac.uk/data_request/cif.

[14] Crystal data of **7e**: formula: $C_{1.74}H_{1.56}O_{0.07}$; M_r: 23.66; temperature: 296(2) K; wavelength: 0.71073 A; crystal system, space group, triclinic, $P\bar{1}$; unit cell dimensions: $a=10.7752(2)$, $b=12.1157(2)$, $c=15.6991(3)$ Å; $\alpha=81.8540(10)$, $\beta=86.4030(10)$, $\gamma=65.3660(10)°$; volume: 1844.16(6) Å^3; $Z=54$; $\rho_{calcd}=1.150$ Mg m^{-3}; μ: 0.069 mm^{-1}; $F_{000}=680$; crystal size: $0.37\times0.25\times0.13$ mm; θ range for data collection: 1.86–25.01°; limiting indices: $-12\leq h\leq 9$, $-14\leq k\leq 14$, $-18\leq l\leq 18$; final R indices $[I>2\sigma(I)]$, $R1=0.0434$, $wR2=0.1032$, R indices (all data): $R1=0.0901$, $wR2=0.1324$. CCDC-731461 contains the supplementary crystallographic data for **7e**. These data can be obtained free of charge from The Cambridge Crystallographic Data Centre via www.ccdc.cam.ac.uk/data_request/cif.

[15] a) P. Hohenberg, W. Kohn, *Phys. Rev.* **1964**, *136*, B864–B871; b) W. Kohn, L. J. Sham, *Phys. Rev.* **1965**, *140*, A1133–A1138.

[16] Gaussian 03, Revision D.01, M. J. Frisch, G. W. Trucks, H. B. Schlegel, G. E. Scuseria, M. A. Robb, J. R. Cheeseman, J. A. Montgomery, Jr., T. Vreven, K. N. Kudin, J. C. Burant, J. M. Millam, S. S.

Iyengar, J. Tomasi, V. Barone, B. Mennucci, M. Cossi, G. Scalmani, N. Rega, G. A. Petersson, H. Nakatsuji, M. Hada, M. Ehara, K. Toyota, R. Fukuda, J. Hasegawa, M. Ishida, T. Nakajima, Y. Honda, O. Kitao, M. J. Frisch, H. Nakai, M. Klene, X. Li, J. E.Knox, H. P. Hratchian, J. B. Cross, C. Adamo, J. Jaramillo, R. Gomperts, R. E. Stratmann, O. Yazyev, A. J. Austin, R. Cammi, C. Pomelli, J. W. Ochterski, P. Y. Ayala, K. Morokuma, G. A. Voth, P. Salvador, J. J. Dannengerg, V. G. Zakrzewski, S. Dapprich, A. D. Daniels, M. C. Strain, O. Farkas, D. K.Malick, A. D. Rabuck, K. Raghavachari, J. B. Foresman, J. V. Ortiz, Q. Cui, A. G. Baboul, S. Clifford, J. Cioslowski, B. B. Stefanov, G. Liu, A. Liashenko, P. Piskorz, I. Komaromi, R. L. Martin, D. J. Fox, T. Keith, M. A. Al-Laham, C. Y. Peng, A. Nanayakkara, M.Challacombe, P. M. W. Gill, B. Johnson, W. Chen, M. W. Wong, C. Gonzalez, J. A. Pople, Gaussian, Inc., Wallingford CT, **2004**.

[17] a) A. D. Becke, *Phys. Rev. A* **1988**, *38*, 3098–3100; b) A. D. Becke, *J. Chem. Phys.* **1993**, *98*, 1372–1377 and 5648–5652; c) C. Lee, W. Yang, R. G. Parr, *Phys. Rev. B* **1988**, *37*, 785–789.

[18] a) M. T. Cances, B. Mennucci, J. Tomasi, *J. Chem. Phys.* **1997**, *107*, 3032–3041; b) M. Cossi, V. Barone, B. Mennucci, J. Tomasi, *Chem. Phys. Lett.* **1998**, *286*, 253–260.

[19] a) E. G. Bakalbassis, S. Spyroudis, E. Tsiotra, *J. Org. Chem.* **2006**, *71*, 7060–7062; b) S. Y. Gu, M. D. Su, *J. Phys. Chem. A* **2007**, *111*, 6587–6591; c) R. M. Moriarty, S. Tyagi, D. Ivanov, M. Constantinescu, *J. Am. Chem. Soc.* **2008**, *130*, 7564–7565.

Received: November 15, 2009
Published online: March 22, 2010

